in Molecular & Cellular Proteomics (accepted 18/07/2016) available at doi:10.1074/mcp.M116.060681

Comparative proteomics and functional analysis reveal a role of *P. falciparum* osmiophilic bodies in malaria parasite transmission

Pablo Suárez-Cortés[1], Vikram Sharma[2], Lucia Bertuccini[3], Giulia Costa[4], Naa-Lamiley Bannerman[2], Anna Rosa Sannella[1], Kim Williamson[5], Michael Klemba[6], Elena A. Levashina[4], Edwin Lasonder[2], Pietro Alano[1*]

1: Dipartimento di Malattie Infettive, Parassitarie ed Immunomediate, Istituto Superiore di Sanità, Viale Regina Elena n.299, 00161 Roma, Italy.

2: School of Biomedical and Healthcare Sciences, Plymouth University, Drake Circus, Plymouth, Devon, UK.

3: Dipartimento Tecnologie e Salute, Istituto Superiore di Sanità, Viale Regina Elena n.299, 00161 Roma, Italy.

4: Department of Vector Biology, Max-Planck Institute for Infection Biology, Charitéplatz 1, 10117 Berlin, Germany.

5: Department of Biology, Loyola University, 1032 West Sheridan Road, Chicago, IL 60660, USA.

6: Department of Biochemistry, Virginia Tech, Blacksburg, VA, USA 24061

*: To whom correspondence should be addressed. Tel.: 39-064990-2868; Fax: 39-064990-2226; E-mail: alano@iss.it.

Running title: Functional proteomics of *P. falciparum* osmiophilic bodies

Keywords: Plasmodium; parasite transmission; gametocyte; osmiophilic bodies; Anopheles mosquito infection

Abbreviations: RBCs : Red Blood Cells; OBs: Osmiphilic Bodies; PVM: Parasitophorous Vacuole Membrane; 5-FCT: 5-fluorocytosine; GFP: Green Fluorescent Protein; WGA: Wheat Germ Agglutinin; XA: Xanthurenic Acid; PFA: Parafomaldehyde; SD: Standard Deviation; FDR: False Discovery Rate; LFQ: label free quantification; WB: Western Blot; IFA: Immunofluorescence Assay; OBC: Osmiophilic Body Candidate; BF: Bright Field

SUMMARY

An essential step in the transmission of the malaria parasite to the Anopheles vector is the transformation of the mature gametocytes into gametes in the mosquito gut, where they egress from the erythrocytes and mate to produce a zygote, which matures into a motile ookinete. Osmiophilic bodies are electron dense secretory organelles of the female gametocytes which discharge their contents during gamete formation, suggestive of a role in gamete egress. Only one protein with no functional annotation, Pfg377, is described to specifically reside in osmiophilic bodies in *Plasmodium falciparum*. Importantly, Pfg377 defective gametocytes lack osmiophilic bodies and fail to infect mosquitoes, as confirmed here with newly produced *pfg377* disrupted parasites.

The unique feature of Pfg377 defective gametocytes of lacking osmiophilic bodies was here exploited to perform comparative, label free, global and affinity proteomics analyses of mutant and wild type gametocytes to identify components of these organelles. Subcellular localization studies with fluorescent reporter gene fusions and specific antibodies revealed an osmiophilic body localization for four out of five candidate gene products analyzed: the proteases PfSUB2 (subtilisin 2) and PfDPAP2 (Dipeptidyl aminopeptidase 2), the ortholog of the osmiophilic body component of the rodent malaria gametocytes PbGEST and a previously non-annotated 13 kDa protein.

These results establish that osmiophilic bodies and their components are dispensable or marginally contribute (PfDPAP2) to gamete egress. Instead, this work reveals a previously unsuspected role of these organelles in *P. falciparum* development in the mosquito vector.

INTRODUCTION

Each year more than 200 million people suffer from malaria, with an estimated death toll of 438.000 in 2015 (1). Malaria is caused by apicomplexan parasites of the Plasmodium genus, with *Plasmodium falciparum* being the most deadly of the five species capable of infecting humans.

Malaria infection in humans is initiated by the bite of an infected *Anopheles* mosquito, which inoculates hundreds of sporozoites that migrate into the blood stream to reach the liver hepatocytes. Inside the hepatocytes, the parasites multiply asexually yielding thousands of hepatic merozoites which invade red blood cells (RBCs). Blood stage asexual parasites undergo indefinite cycles of merozoite proliferation, egress from the host cell and reinvasion of new RBCs, causing malaria symptoms. During asexual growth, a fraction of parasites enter sexual differentiation (gametocytogenesis). This process takes place in the bone marrow where the parasites go through five morphologically distinct stages, culminating after 10 days in the formation of the falciform mature gametocytes. Mature sexual stage parasites are then released into the peripheral blood stream where they are ready to be taken up by mosquitoes during the next insect blood meal.

In the mosquito midgut mature female and male gametocytes react to several physical and chemical factors (2), transforming into male and female gametes. Gametogenesis begins with the rapid rounding-up of the elongated parasites and ends in 15-20 minutes with the egress of gametes from erythrocytes, each male gametocyte producing eight flagellated microgametes and each female forming a single spherical macrogamete. After fertilization, the zygote transforms into an ookinete, which traverses the mosquito midgut epithelium to develop into an oocyst, producing several thousand sporozoites able to migrate to the mosquito salivary glands, ready to infect a new human host (3).

Apicomplexan parasites invade and egress from different cellular types. These complex processes are orchestrated by diverse factors produced by the sets of membranous secretory organelles found in all parasite developmental stages. Conservation of the secretory organelles among apicomplexa highlights the importance of these structures in the life cycle of these diverse parasites.

In Plasmodium, the family of apical secretory organelles include rhoptries, micronemes and dense granules. Rhoptries are elongated paired organelles found in merozoites, while micronemes, smaller in size, are present in merozoites, sporozoites and ookinetes. These organelles secrete factors that mediate host cell invasion and egress. Finally, spherical dense granules are found in the merozoites, where they contribute to the formation of the parasitophorous vacuole after RBC invasion (4–6). Identification of specific organellar components recently enabled the definition of other secretory organelles such as mononemes and exonemes. The mononeme is a thread-like compartment hosting the PfROM1 protein, important in invasion (7), while exonemes, similar in shape and distribution to micronemes, release their contents that are indispensable to merozoite egress, e.g. the subtilisin like protease PfSUB-1(8).

Protein content of these organelles has been identified mainly by cell fractionation experiments where differential and/or gradient centrifugation yielded protein samples enriched in the target organelle. The difficulty in isolating purified individual organelles however made it essential to confirm the localization of the identified candidate proteins, usually by subcellular localization analyses with specific antibodies or transgenic reporter gene fusions.

Sexual blood stages of Plasmodium retain another type of secretory organelles, the osmiophilic bodies (OBs). In *P. falciparum*, elongated OBs (about 200nm in diameter) are detected in the periphery of stage III gametocytes (predominantly female) from day four of gametocyte maturation. In the murine malaria model *Plasmodium berghei* OBs of smaller size are described in female gametocytes and a class of morphologically distinct OBs has been recently described

in male gametocytes (9). Very little information is currently available on the protein content of these organelles. The first to be identified and the only specific protein of the *P. falciparum* OBs to date is Pfg377 (10). Three OB specific proteins have been identified in *P. berghei*, Pbg377; Male Development-1 (PbMdv-1) and Gametocyte Egress and Sporozoite Traversal (PbGEST) (11,12). While Pbg377 and Pfg377 localize to OBs in *P. berghei* and *P. falciparum*, respectively, PbMdv-1 is specific to OBs only in *P. berghei*, whereas its *P. falciparum* homologue has a broader distribution in several gametocyte-derived membranes (13,14). Finally, the localization of the PbGEST orthologue has not been characterized yet in the human malaria parasite.

Previous observations that OBs are discharged, probably into the PVM, at the start of gametogenesis and that are no longer present in extracellular gametes suggested a function of these organelles in gamete egress from the RBCs. Consistently, disruption of either Pfg377, PbMdv1 and PbGEST in transgenic parasites resulted in a mild defect in efficiency and/or a delay in gamete egress (9-12). In *P. falciparum*, recent studies however questioned the involvement of OBs and Pfg377 in gamete egress (15), attracting attention to the additional phenotypes described in the *pfg377*KO sexual stages, namely that the Pfg377-defective gametocytes are almost completely depleted of OBs, and that their capacity to infect mosquitoes is virtually abolished (16). Interestingly, in *P. berghei*, the *pbg377* gene disruption resulted in a reduction in size, but not in number, of OBs in gametocytes, and no significant reduction in mosquito infectivity (9), suggesting existence of species specific difference.

The lack of OBs in the Pfg377-deficient *P. falciparum* gametocytes constitutes to our knowledge an almost unique case of a parasite developmental stage depleted of a specific organelle. An analogous situation was observed only with the loss of the apicoplast in the *P. falciparum* asexual stages after a treatment with fosmidomycin, an isoprenoid precursor biosynthesis inhibitor (17).

The work presented here exploited the lack of OBs in Pfg377-deficient gametocytes to identify OB protein content by two label free quantitative proteomic approaches, a global comparative

proteomics analysis and an affinity proteomics approach identifying Pfg377 interacting proteins. Functional studies on selected candidate gene products revealed an OB localization for four out of five identified proteins, including two proteases, and the persistence of OB components in gametes after egress from the RBC. These results identify a functional role of OBs in parasite development and transmission in the Anopheles vector.

EXPERIMENTAL PROCEDURES

Experimental Design and Statistical Rationale - The objective of this experiment is to identify osmiophilic body proteins expressed in gametocytes by a cellular comparative proteomics approach between wild type (*wt*) gametocytes and gametocytes depleted of osmiophilic bodies, and by an affinity proteomics approach identifying Pfg377 interaction partners in *wt* gametocytes and gametocytes depleted of osmiophilic bodies. Control, *wt* gametocyte and Pfg377-depleted gametocyte samples were produced by culturing *P. falciparum* parasites in human red blood cells. For each sample, three biological repeats were cultured independently resulting in 3 samples for *wt* gametocytes, and in 6 samples for Pfg377-depleted gametocytes. These samples were studied by an gel-LC MS/MS approach (Fig. S2), and proteins were identified by searching tandem mass spectrometry data against a protein database composed of *P. falciparum* and human proteins. Protein abundances were estimated by label free quantification (LFQ) based on peptide intensities in MaxQuant. Gametocyte protein abundance data was then filtered to include proteins that are quantified across all samples, that are upregulated in mature gametocytes (30) and that are upregulated in female gametocytes with female/male protein ratio > 1.2 (18).

Statistical significant differences in protein levels between *wt* gametocyte and Pfg377 depleted gametocytes was determined by Student t tests comparing *wt* group (3 expression data sets) versus sample groups (6 expression data sets).

For the affinity proteomics experiment single biological repeats were used for measuring protein interaction partners of Pfg377 in *wt* gametocytes and Pfg377-depleted gametocytes by immunopurification and LC-MS/MS.

The results of the cellular comparative proteomics approach and the affinity proteomics approach were combined to generate a list of putative osmiophilic body proteins.

Plasmodium falciparum culture – P. falciparum clone 3D7 was used throughout (19). Wild type and transgenic lines were cultured in O+ human red blood cells at 5% haematocrit in RPMI 1640 plus hypoxanthine 50 µg/ml, HEPES 25 mM, 0.225% sodium bicarbonate and 10 mg/ml gentamicin, supplemented with 10% heat inactivated human serum. Parasites were kept at 37°C, in a 2% O, 5% CO2 and 93% N_2 atmosphere. For gametocyte production, asynchronous parasites were grown to high parasitaemia (>8%) and culture medium was doubled at this point. The day after, medium was changed and N-acetylglucosamine 50 mM added. N-acetylglucosamine was maintained for five days, until no asexual parasites were detected in the culture. Stage II gametocytes were detected 48 hours after the addition of N-acetylglucosamine while mature stage V gametocytes appeared nine days after the start of the treatment. Percoll and MACS purification of gametocytes was performed as described (20). Protocols used to thaw and freeze parasites are described elsewhere (21). In the production of gametocytes for mosquito experimental infections, N-acetylglucosamine and gentamicin were omitted from culture medium not to interfere with the mosquito microbiome.

Production of transgenic parasites - Ring stage parasites at 2–3% parasitaemia were transfected by electroporation with 80–100 µg of transfection vectors using the following conditions: voltage: 0.31 kV, capacitance: 960 mF, resistance to infinity (22). Transfected parasites were then added to 5 ml of fresh media, 5% haematocrit. Parasites were cultured without drug selection for 24 hours and WR99210 5nM was then added. Medium was renewed every day during the first 4 days, and every two days after that. Fresh 1% haematocrit RBCs

were added every 7 days until resistant parasites appeared, which happened from 14 days after transfection. Rounds of drug cycling consisting of 21 days of growth in drug absence before reintroduction of drug pressure were carried out to enrich the population of parasites with integrated plasmid (22).

To produce *pfg377*KO parasite lines, plasmid pHH-TK-*pfg377* (Fig. S1) was transfected as described above and WR99210 (positive) and ganciclovir (negative) selections were applied to obtain lines GT5 and GT8 from independent transfections. After Southern blot analysis confirmed disruption of the *pfg377* locus (Fig. S1), clones were obtained by limiting dilution. Parasite clones 5-2 and 8-20, from the GT5 and GT8 lines respectively, were used in this work.

In other experiments, selection for plasmid chromosomal integration was achieved through cycles of off-drug (one week)/on-drug. In the case of KO plasmids, negative selection was then performed adding 40 μM 5-fluorocytosine (5-FCT) to the medium (23). Parasites resistant to both WR99210 and 5-FCT appeared in Giemsa smears after a week. GFP tagged and KO lines were then cloned by limiting dilution (19).

Morphometric analysis of OB size in wt and pfg377KO gametocytes - Micrographs of ultrastructure sections of *wt* and *pfg377KO* mature gametocytes were used to count and measure the size of OBs. The eccentricity (e) of OBs in the *wt* and in the *pfg377*KO gametocytes was calculated according to the formula $e = \sqrt{1 - \frac{b^2}{a^2}}$. Student's t test was performed to determine if (e) values were significantly different in *wt* and *pfg377*KO OBs.

Measurement of gametocyte egress efficiency - Egress efficiency of gametes was measured as described previously (15). Briefly, mature gametocyte cultures were stained with fluorophore-bound WGA (5μg/ml), which binds to RBCs surface, and then gametogenesis was triggered by adding 20μM xanthurenic acid (XA). After 15 minutes at room temperature parasites were fixed in 1% paraformaldheide (PFA) and mounted in microscope slides. Gametes were identified and the presence or absence of RBC was assessed examining

presence or absence of the fluorescence surrounding the parasites. For each parasite line/clone, at least 4 independent experiments were done, counting 200 gametes in each case. T-tests were performed on individual pairs of *wt*-KO parasites.

Mosquito Rearing and Parasite Infections - *Anopheles gambiae* Ngousso mosquitoes used throughout the study were maintained at 29°C 70%–80% humidity 12/12 h day/night cycle. Mosquitoes were fed on gametocytes cultured in O+ human red blood cells (Haema, Berlin) through a membrane feeder at 37°C for 15 min. 3D7 wild type and *pfg377*KO clone 5-2 gametocyte cultures were adjusted for approximately the same final stage V gametocytaemia (0,03-0,1%) in each experiment repeat. Unfed mosquitoes were removed shortly after infections, while fed mosquitoes were maintained at 26°C in a secured S3 laboratory according to the national regulations (Landesamt für Gesundheit und Soziales, project number 411/08). Oocysts were counted in the dissected midguts11 days post infection.

Gametocyte purification for proteomic analysis - Three biological replicates of this experiment were performed. Magnetic purification with CS columns in a MaxiMACS (Miltenyi Biotec) was used to purify the gametocytes from non-infected RBCs. Prior to purification, Giemsa smears were analyzed to measure gametocyte stage synchronicity and sex ratios and control for the absence of asexual parasites or immature gametocytes. Purified parasites were counted using a cell counter chamber, and $2x10^7$ parasites were pelleted and frozen for each sample. Parasites were lysed in 4% SDS in PBS, 4X Laemmli Sample Buffer, and reduced with 50 mM DTT at 95 ^{0}C for 5 minutes prior to protein gel electrophoresis.

Gametocyte sample preparation for LC-MS/MS Experiments - Gel based fractionation of the proteins prior to tryptic digestion was conducted by gel electrophoresis using 10 % Criterion XT Bis-Tris precast gels (Biorad inc, UK) and XT-MES running buffer pH 6.4. Gels were stained with Colloidal Coomassie Blue (Severn Biotech), and divided into 6 slices per lane. Gel slices were treated with 10 mM DTT and 55 mM iodoacetamide and digested by trypsin overnight at

37 ^{0}C as described previously (24). Tryptic digests were acidified to a final concentration of 0.1% TFA and purified by STAGE tips (25).

Liquid chromatography tandem mass spectrometry - Ultimate 3000 UPLC (Thermo Fisher, Germany) connected to the Orbitrap Velos Pro mass spectrometer (Thermo Fisher, Germany) was used to perform tandem mass spectrometry experiments. Peptides were loaded on a 2 cm Acclaim™ PepMap™100 Nano-Trap Column (Thermo Fisher, Germany) and were separated by a 25 cm Acclaim™ PepMap™100 Nano LC column (Thermo Fisher, Germany) packed with 3 µm C18 beads. Sample run with a flow-rate of 300nl/min in a 120 min gradient of 95% buffer A/5% buffer B to 65% buffer A /35 % buffer B (buffer A: 0.5% acetic acid. Buffer B: 0.5% acetic acid in 100% acetonitrile). Peptides eluting from the column were electrosprayed into the mass spectrometer at 2.3 kV pray voltage. Orbitrap was used for data acquisition in a data-dependent mode automatically switching between MS and MS2. Orbitrap cell was used to acquire full-scan spectra of intact peptides (m/z 350-1500) with automated gain control accumulation value of 1.000.000 ion, with a resolution of 60.000. The ten most abundant ions were then sequentially isolated and fragmented in the linear ion trap, where dissociation was induced through collision, using an accumulation target value of 10.000, a normalized collision energy of 32% and a capillary temperature of 275°C. Dynamic exclusion of ions sequenced within the 45 previous seconds was applied. Unassigned charge states and singly charged ions were excluded from sequencing. For MS2 selection, a minimum of 10.000 counts was required.

Peptide identification and quantification by MaxQuant - Andromeda (26) search engine integrated in the MaxQuant (Version 1.3.0.5) (27) was used to identify proteins. Peak lists were generated for the top 6 most intense MS peaks in 100 Da windows by MaxQuant prior to the database search. The protein database contained 91,901 protein sequences from *P. falciparum* (http://plasmodb.org/common/downloads/release-27/Pfalciparum3D7/) and human IPI version 3.68 (ftp://ftp.ebi.ac.uk/pub/databases/IPI/) supplemented with frequently observed contaminants. Andromeda search parameters for protein identification were set to tolerance of 6

ppm for the parental peptide and 0.5 Da for fragmentation spectra and trypsin specificity allowing up to 2 miscleaved sites. Deamination of glutamine, oxidation of methionine, and asparagine and protein N-terminal acetylation were set as variable modifications, carboxyamidomethylation of cysteines was specified as a fixed modification. Minimal required peptide length was specified at 6 amino acids. MaxQuant was used as described (27) to perform internal mass calibration of measured ions and peptide validation by the target decoy approach and to enable the 'match between run option' for an elution time window of 2 minutes. Peptides and proteins detected by at least two peptides in one of the samples with a false discovery rate (FDR) of 1% were accepted. Excluded from validation were proteins identified by site only, external contaminants and reversed proteins. Proteins were quantified by normalized summed peptide intensities (28,29) computed in MaxQuant with the label free quantification (LFQ) option switched on.

Identification of osmiophilic body proteins by global proteomics - Osmiophilic body proteins were identified by a comparison in protein abundances between *wt* gametocytes and *pfg377*KO gametocytes. To minimize variability from differences between parasites strains, gametocyte samples from two independent *pfg377*KO parasite strains and from *wt* gametocytes were cultured in parallel. A total of three biological replicate samples were generated and analyzed. Morphological analysis of the samples ensured similarity across them through evaluation of absence of asexual parasites, sex ratio, maturity, percentage of infected RBCs and percentage of gametes. Mass spectrometry data were acquired sequentially, completing the acquisition of data from each batch individually before the analysis of subsequent samples. Data from each sample was acquired in triplicate and processed by MaxQuant.

Perseus (Version 1.3.7.1) (30) was used to perform statistical analysis for the identification of a list of putative osmiophilic body proteins. Prior to analysis in Perseus the gametocyte protein abundance data was filtered to include proteins that are quantified across all samples, that are upregulated in mature gametocytes (31) and proteins that are upregulated in female

gametocytes with female/male protein ratio > 1.2 (18). Protein abundance data was normalized by median expression values and transformed to relative expression data for each biological repeat and subsequently imported into Perseus and classified into a group of *pfg377*KO gametocyte samples and a group of wild type gametocytes. Statistical significant differences between both groups were calculated by two-tailed t-tests with results presented in a Volcano plot depicting protein ratios versus statistical significance.

The mass spectrometry proteomics data have been deposited to the ProteomeXchange Consortium via the PRIDE (32) partner repository with the dataset identifier PXD004124.

Identification of osmiophilic body proteins by affinity proteomics - Prior to the immunopurification experiment, antibodies against Pfg377 B fragment were crosslinked to agarose beads: Agarose beads (50μL) were washed 3 times with PBS 0.1% Tween-20 (Sigma-Aldrich) and resuspended in 100 mM HCl, 0.5 M NaCl (pH 8.0). Antibodies (20μL) were added and the mix incubated for 3h at room temperature. Beads were then washed (500g centrifugations for 5 minutes was performed to pellet beads throughout the experiment) three times with 200mM sodium borate pH9.0 to eliminate unbound antibody. Beads were then resuspended in 3 volumes of methylpimelimidate (DMP, the crosslinking agent) 20mM in 200mM borate pH9.0 and incubated for 90 minutes at room temperature in a shaker. Crosslinking solution was washed away and beads resuspended washed 3 times in TrisHCl 50mM pH7.5, and then incubated at room temperature for 2 hours, to terminate the crosslinking reaction. Non-crosslinked antibodies were removed by washing 3 times with 1mL of 0.58% v/v acetic acid 150mM NaCl. Beads were then washed 3 times in PBS and stored at 4° until experiment began. Correct crosslinking was evaluated through an acrylamide protein gel in which crosslinked beads showed to contain a protein of the expected length of the α-Pfg377B antibodies.

Samples containing $3x10^7$ mature synchronous gametocytes from *wt* and the *pfg377*KO clone 8-20 were isolated via magnetic columns, pelleted and frozen. Lysis occurred for 30 minutes at 4°C in lysis buffer (50mM Tris-HCl pH7.5, 150mM sodium chloride, 1% Nonidet P40 (Sigma-Aldrich), 0.5% sodium deoxycholate, Complete protease inhibitor (Roche)). Debris was pelleted and supernatants were incubated for 3 hours at 4°C with non-crosslinked agarose beads to pre-clear the lysate of proteins binding to immuno-beads in a non-specific manner. Non-crosslinked beads were pelleted and discarded, and pre-cleared supernatant was then incubated overnight at 4°C with α-Pfg377B-crosslinked beads, to allow the binding of Pfg377 and any associated proteins to the specific antibodies. Beads were then pelleted and washed three times in lysis buffer. Elution of the bound proteins was achieved through addition of 2x Laemmli sample buffer (Life Sciences) to the beads and incubating the sample at 95°C for 5 minutes. Beds were centrifuged and the supernatant containing the purified proteins used in subsequent steps. Gel based fractionation of the proteins in the supernatants was conducted by gel electrophoresis in a 4%-12% Bis-Tris precast gel (Life Technologies) and MES-SDS buffer. The gel was stained with Colloidal Coomassie Blue and a single slice containing each sample was excised. Gel slices were treated with 10 mM DTT and 55 mM iodoacetamide and digested by trypsin overnight at 37 ^{0}C as described previously (24). Tryptic digests were acidified to a final concentration of 0.1% TFA and purified by STAGE tips (25).

Immuno-purified complexes of Pfg377 binding proteins in *P. falciparum wt* gametocytes were measured with liquid chromatography tandem mass spectrometry and analyzed by MaxQuant as described above. Immuno-purified complexes of Pfg377 binding proteins in *P. falciparum pfg377*KO gametocytes functioned as negative controls. Protein abundance data (LFQ) was loaded into Perseus for further analysis, where only proteins detected with at least 2 razor peptides in one of the samples and detected in more than 50% of the samples were considered. Missing LFQ data were imputed with intensities from the lower part of normal data distribution, with an imputation with of 0.3 and a shift of 0.8. Proteins showing LFQ *wt*/LFQ KO ratio > 30

were considered as candidates. Ribosomal proteins, a common non-specific contamination in affinity purification, were ignored as candidates.

The mass spectrometry proteomics data have been deposited to the ProteomeXchange Consortium via the PRIDE (32) partner repository with the dataset identifier PXD004088

RESULTS

Depletion of osmiophilic bodies in Pfg377-defective gametocytes does not affect their egress from erythrocytes but compromises their infectivity to mosquitoes – As some reversion to *wt* was reported in the previously described *pfg377* knock out (*pfg377*KO) parasites (16), new independent *pfg377* defective parasites were obtained through gene disruption by double crossover recombination. Two parasite clones, *pfg377*KO 5-2 and 8-20, were derived from independent transfections and the structure of the *pfg377* disrupted locus was confirmed by molecular analysis (Fig. S1). Inspection of independent ultrastructure sections from stage IV–V gametocytes from clones 5-2 and 8-20 confirmed that gametocytes defective in the production of Pfg377 are depleted of OBs (Fig. 1A) (16). In addition, a morphometric analysis on the residual electron dense granules in the Pfg377-defective gametocytes revealed differences in both the size and the shape of these organelles from those observed in *wt* gametocytes, being smaller and lacking the typically elongated shape (Table S1). Immunofluorescence (IFA) and Western blot (WB) analyses with αPfg377 antibodies confirmed disruption of Pfg377 expression in the late gametocyte stages of the *pfg377*KO clones (Fig. 1B, C).

As the observed reduction in efficiency to egress erythrocytes of the Pfg377-defective gametes described in (16) was not reproduced in subsequent experiments (15), this phenotype was analyzed also in the newly obtained *pfg377*KO gametocytes. Again, no difference in gametocyte egress efficiency was detected between *wt* and *pfg377*KO (Fig. 1D), thereby confirming that Pfg377 is dispensable for gametocyte egress.

To investigate whether *pfg377* disruption affected developmental steps after gamete egress, transmission of the *pfg377*KO clone 5-2 to mosquitoes was analyzed in experimental infections of *Anopheles gambiae*. Striking decrease in the prevalence of infection and in the number of developing oocysts was observed for *pfg377*KO parasites, indicating that OBs are required for *Plasmodium* transmission (Fig. 1E; Table S2).

In summary, these experiments demonstrated that Pfg377 defective sexual stages egress normally from erythrocytes at gametogenesis, despite lacking their complement of OBs, and confirmed a severe defect in mosquito infectivity, thus revealing an unsuspected role of OBs and/or the OB specific Pfg377 protein in mosquito stages after gamete egress.

Comparative proteomics of wt *and* pfg377*KO gametocytes identifies candidates for organelle resident proteins* - Attempts to isolate or to enrich for OBs in gametocyte cell fractionation experiments from *wt* parasites in order to identify resident proteins by mass spectrometry were unsuccessful (data not shown). As *pfg377*KO gametocytes are virtually depleted in OBs, this opportunity was exploited to isolate OB proteins by a comparative mass spectrometry analysis between *wt* and OB defective gametocytes. The underlying assumption of this experiment was that OB proteins failing to be trafficked to these organelles may be degraded and consequently underrepresented in the proteome of the defective gametocytes.

Three biological replicates of this experiment were performed, using, in each case, parallel synchronous gametocyte samples from *wt* and both independent *pfg377*KO clones. Prior to gametocyte purification for mass spectrometry analysis, morphological examination confirmed that stage of maturation, sex ratio and fraction of spontaneously activated 'rounded-up' parasites were similar in the *wt* and the *pfg377*KO gametocyte cultures (data not shown).

Gametocyte extracts from the nine samples were analyzed by label free quantitative proteomics (29). Briefly, parasite protein extracts were fractionated through gel electrophoresis, trypsin-digested and purified with Stage tips. Samples were then analyzed by LC MS/MS and mass spectrometry data was processed with MaxQuant by the procedure depicted in Fig. S2. This resulted in the identification of 29,904 unique *P. falciparum* peptide sequences (Table S3) mapping to 1942 protein groups in all gametocyte samples (Table S4). This protein set was filtered for proteins described to be upregulated in stage V gametocytes vs stage I (31) and upregulated in female vs male gametocytes (18) since OBs appear on day four of sexual

differentiation and accumulate in female gametocytes (33). Differential protein expression in the resulting list of 386 proteins (Table S5) between *wt* gametocytes and OB depleted gametocytes was determined by Student's t tests and visualized by a Volcano plot, where statistical significance is plotted versus protein ratios (Fig. 2). This analysis identified 16 potential OB protein candidates (OBCs) significantly enriched in *wt* gametocytes compared to the *pfg377*KO parasites (Table 1). This list includes as expected Pfg377, reduced more than 1000 fold in the *pfg377*KO gametocytes compared to *wt*.

In a second comparative proteomics approach, immunopurified Pfg377 complexes were obtained in *wt* and OB-depleted gametocytes to identify Pfg377 interaction partners in *wt* gametocytes as candidates for OB associated proteins. The mass spectrometric analysis of the purified Pfg377 complexes identified 462 unique *P. falciparum* peptide sequences (Table S6) mapping to 66 protein groups (Table S7). The comparative proteomics analysis revealed 3 proteins overrepresented more than 30 fold in the *wt* samples: the bait protein Pfg377, as expected; PfPSOP12, which was identified also in the global comparative approach described above and PF3D7_1214800, a hypothetical 13kDa protein.

Altogether, the two comparative proteomic approaches identified 16 parasite gene products as putative OBCs. Five OBCs were chosen for further characterization based on (i) their conservation in *P. berghei* (PfGEST); (ii) the results of the immunopurification experiments (the 13 kDa protein PF3D7_1214800, named hereafter OBC13, and PfPSOP12, which was identified also in the global proteomics approach), and (iii) the potential role in proteolysis revealed by functional annotation (PfSUB2 (Subtilisin 2) and PfDPAP2 (Dipeptidyl aminopeptidase 2).

All of these proteins display a predicted transmembrane domain and a signal peptide. Additionally, the selected genes show similar transcriptional profiles to that of *pfg377*, indicating functional association of the OBC proteins (34) (Fig S3).

PfGEST is a conserved component of the gametocyte osmiophilic bodies in human and rodent malaria parasites - An antibody against the C-terminal portion of PfGEST was produced and used to study the localization of this protein in gametocytes (Fig. S4). In WB analysis, the α-PfGEST antibody specifically reacted with a band of the expected molecular weight of approximately 25 kDa in samples from gametocytes and its intensity increased in stage V gametocytes as compared to the immature stage II-III (Fig. 3A). The band was not observed in extracts from equivalent number of uninfected red blood cells (RBCs) or asexual parasites. This antibody was used to investigate the PfGEST subcellular localization by IFA and immuno-electron microscopy analyses on stage IV-V gametocytes. In IFA, conspicuous α-PfGEST positive signal co-localized with the specific granular fluorescent pattern obtained with antibodies against the OB marker Pfg377, strongly indicating that PfGEST resides in these organelles (Fig. 3B). This was confirmed by immuno-electron microscopy, where the α-PfGEST-reactive colloidal gold particles were detected inside or on OBs (Fig. 3C).

These results demonstrate PfGEST presence in the OBs. However, detection of PfGEST in Pfg377 negative gametocytes, the male sexual stages that lack OBs, suggests that distribution of this protein is not restricted to OBs and that it may be present in other membranous structures (Fig. S5).

Functional analysis identifies new protein constituents of the osmiophilic bodies - To investigate the subcellular localization of the identified OBC proteins, reporter gene fusions between the coding sequences of respective genes and Green Fluorescent Protein (GFP) were generated and transfected in 3D7 parasites. Four lines were obtained, whose endogenous chromosomal loci were successfully tagged by the fluorescent reporter (Fig. S6). Clonal lines *pfsub2GFP, pfdpap2GFP and pfobc13GFP* and the uncloned line *pfpsop12GFP* were used for further analysis. GFP expression of the tagged proteins was first investigated in live asexual blood

stages and gametocytes. In asexual stages, fluorescence was observed only in schizonts of the *pfsub2GFP* clone. Further experiments on these parasites showed a full co-localization of the GFP signal with that from α-PfAMA1 antibodies on the merozoite apical portion, which confirmed that the PfSUB2GFP fusion is correctly trafficked and localized in asexual stages (Fig. S7). The analysis of live stage V gametocytes from all GFP tagged lines showed a weak but appreciable granular GFP fluorescence only in gametocytes from the 3D7*pfsub2GFP* and the 3D7*pfdpap2GFP* clones (Fig. 4A), whilst fluorescence of the *pfobc13GFP* and *pfpsop12GFP* gametocytes was barely detectable.

To increase detection levels of the reporter proteins, IFA experiments were performed with antibodies against the GFP reporter, used alone or in combination with those against the OB marker Pfg377 and the newly identified OB component PfGEST. The α-GFP antibody produced a granular fluorescence pattern in gametocytes of the *pfsub2GFP, pfdpap2GFP* and *pfobc13GFP* lines (Fig. 4B, left). A different pattern was found instead in the *pfpsop12GFP* line, with gametocytes showing in some experiments a more condensed cytoplasmic signal, or no signal at all (data not shown). Importantly, the GFP signals in the gametocytes of 3D7*pfsub2GFP,* 3D7*pfdpap2GFP* and 3D7*pfobc13GFP* transgenic clones co-localized with those of the OB marker Pfg377 and of PfGEST (Fig. 4B, right, Fig. S8), indicating that all three fusion proteins were present in OBs. In the double IFA with α-Pfg377 and α-GFP antibodies, a quantitative assessment of signal co-localization using the Costes approach (35) confirmed co-localization with Pearson's R values of 0.83±0.16, 0.83±0.13 and 0.85±0.03 in the *pfsub2GFP, pfdpap2GFP* and *pfobc13GFP* gametocytes, respectively. In the *pfsub2GFP* line, available antibodies against a recombinant portion of the PfSUB2 protein (36) were used to confirm the localization of the endogenous protein to the Pfg377-positive structures (Fig. S9). Finally, the above double IFA experiments were conducted using a different combination of antibodies, a mouse αGFP and a rabbit αPfg377 against the B portion of the protein (10) (Fig. S10). These

experiments produced results comparable to those shown in Fig. 4B, confirming co-localization of the GFP tagged OBC proteins with Pfg377.

Importantly, in all experiments the granular patterns of the GFP tagged proteins were observed exclusively in the Pfg377 positive female gametocytes and not in the Pfg377 negative male gametocytes (Fig. S11; Table S8). These results show that, similar to Pfg377, PfSUB2GFP, PfDPAP2GFP and PfOBC13GFP proteins localize specifically to the OBs.

Role of the newly identified OB proteins in gametocyte egress and persistence in the extracellular gametes - To investigate the function of the identified OB proteins in gametogenesis, and more specifically their role in the release of gametes from the infected erythrocyte, a phenotypic analysis was carried out on transgenic parasites where the OB genes were disrupted. This analysis was not possible for PfSUB2, reported to be essential for parasite proliferation (37). Production of *pfdpap2*KO parasites was previously described (38), and parasites disrupted in the *pfobc13* gene were generated for this purpose (Fig S12).

Efficiency of egress of the *pfdpap2*KO and *pfobc13*KO gametes was measured at 15 minutes after induction. While a two-fold decrease in egress efficiency was observed for the *pfdpap2*KO gametes, no difference was observed in the egress of the *pfobc13*KO gametes (Fig. 5).

As no obvious function in gamete egress could be ascribed to two out of three OB proteins analyzed, i.e. Pfg377 and PfOBC13, the fate of the newly identified components of these secretory organelles was investigated after gamete egress. Mature gametocytes from the *pfsub2*GFP, *pfdpap2GFP* and *pfobc13GFP* lines were triggered to undergo gametogenesis and the presence of the fusion proteins was investigated in live extracellular gametes. The signal from the PfSUB2GFP protein was detected in the periphery of gametes at least 30 minutes after egress from RBCs, suggesting a surface localization of the fusion protein. A relatively weaker fluorescence intensity in the extracellular gametes was observed for DPAP2GFP. In contrast,

the OBC13GFP protein was not detected in the egressed gametes, which was expected from the lack of GFP signal in live gametocytes from this line (Fig. 6).

In summary, these analyses indicated that both OB associated proteases PfSUB2 and PfDPAP2 are detectable in extracellular gametes at least 30 minutes after egress from the infected erythrocytes in live extracellular gametes, further substantiating the hypothesis that function of OB proteins may be required for the mosquito stages of parasite development.

DISCUSSION

Although secretory organelles of apicomplexan parasites play key roles in their biology, they remain poorly characterized. This is partially due to the difficulties in their isolation that prevent thorough biochemical analyses. In this work, using *P. falciparum* mutants that lack osmiophilic bodies and comparative proteomics, 16 proteins enriched in *P. falciparum wt* gametocytes were identified and four out of the five analysed were functionally shown to be OB components.

Earlier work suggested that OBs play a role in the gametocyte egress from the red blood cells (16). However, recent studies in *P. falciparum* (15) and *P. berghei* (9) did not confirm this observation. Here, analyses of the newly established independent *pfg377*KO lines confirmed the role of this gene in OBs biogenesis and in parasite transmission to the mosquito vector but not in gamete egress. Results suggest that a block in the parasite development takes place at some point between gametocyte egress and the oocyst maturation in the mosquito midgut. Further studies are needed to elucidate the exact stage at which development of the OBs depleted parasites is arrested.

The almost complete lack of OBs in *pfg377*KO gametocytes was exploited here to develop a comparative proteomic study to identify several new OB proteins. The observed modest differences in the abundance of the OB components PfGEST, PfSUB2, PfDPAP2 and PfOBC13 suggest that *pfg377* deficiency does not impact expression of OB proteins but impairs their trafficking and stability. The comparative proteomics analysis also showed that abundance levels of 26 proteins were increased in the OB-depleted parasites. It is thus possible that the defect in OB biogenesis may cause accumulation of some parasite proteins. Current functional annotation of these proteins did not provide clues on the mechanisms underlying accumulation in the defective gametocytes.

The fact that four out of five candidates analyzed from the list of 16 proteins overrepresented in the *wt* gametocytes were confirmed as OB proteins indicates that this comparative proteomic approach was successful. The exception was represented by PfPSOP12, whose tagged gene product did not co-localize with the signal from α-Pfg377 and α-PfGEST antibodies. This is surprising as this protein was independently identified in both the global comparative proteomics and the co-IP approaches. Moreover, similar to other OBC proteins identified in this study, the ortholog of this protein in the murine parasite *P. berghei*, PbPSOP12, has been detected on the gametocyte surface (39). Therefore, failure to detect PfPSOP12 in OBs could be an artefact of incorrect trafficking of the chimeric GFP-tagged fusion protein and further experiments using anti PfPSOP12 antibodies are needed to clarify this discrepancy.

The localization of proteases PfSUB2 and PfDPAP2 in the gametocyte OBs is intriguing. In asexual parasites, PfSUB2 is expressed in very mature schizonts and trafficked into the merozoite micronemes together with other invasion factors. When micronemes discharge their contents after egress from the host RBC, PfSBU2 relocates to the posterior part of the parasite (40), where its activity during RBC invasion sheds the surface proteins AMA1, MSP1 and PTRAMP from the merozoite surface in a process essential for invasion (41,42). The proteolytic activity of PfSUB2 has been shown to be sequence independent in asexual parasites, which makes it difficult to predict its substrates in sexual stage parasites (37,42). Previous attempts to disrupt PbSUB2 (43) or PfSUB2 have failed (44), suggesting an essential role for the protein in the asexual cycle. Attempts to introduce a GFP-tag in the endogenous gene had also proven unsuccessful (40), with only an HA-tag being successfully inserted into the chromosomal gene locus (41). The discovery of PfSUB2 in the secretory organelles of female gametes presented here open key questions on the role of PfSUB2 in the parasite sexual stages. As a role of the OB content in the release of gametes from the infected erythrocyte membrane seems ruled out, the presence of PfSUB2 in gametes after egress proposes a role for this enzyme in later stages

of the mosquito infection. Interestingly, in *P. berghei* it has been observed that the rodent parasite SUB2 is secreted into the cytoplasm of the mosquito host cells invaded by ookinetes, hinting that this sheddase could have a role in this mosquito stage of the parasite (45). Recent advances in the genetic manipulation of *P. falciparum* (46,47) makes it now conceivable to generate parasites with a conditional PfSUB2 expression to elucidate its function in the different developmental stages.

The other OB protease identified here, PfDPAP2, is expressed only in gametocytes and its possible role in gametocytogenesis has been previously studied (38). PfDPAP2 belongs to the small conserved family of parasite DPAP proteases with PfDPAP1 and PfDPAP3. Phenotypically, DPAP2 defective parasites in the human and in the rodent parasites show a normal gametocytogenesis. The *pbDPAP2*KO parasites were tested for male gamete exflagellation, showing no difference compared to *wt* parasites, and the protease resulted to be not required for mosquito transmission (38). The work presented here reveals that PfDPAP2 is localized in OBs and that its ablation in *pfDPAP2*KO parasites results in a mild defect in gamete egress. Interestingly, this phenotype is the only observation that proposes a relationship between *P. falciparum* OBs and gamete egress. In this respect it is possible that PfDPAP2 has a role similar to that of PfDPAP3, which is localized in the micronemes of the asexual schizont where it processes proteins essential for the egress from RBCs (48).

The PfSUB2, PfDPAP2 and PfOBC13 proteins appear here to be specific components of OBs, as the GFP tagged proteins are not detectable in the Pfg377 negative male gametocytes. In contrast, PfGEST, whose localization in OBs was here confirmed by specific antibody reactivity in immunoelectron microscopy analysis, was also found in male gametocytes. The distinct granular pattern observed also in these gametocytes (data not shown) opens the possibility that

other secretory organelles, negative to Pfg377, exist in *P. falciparum*. One instance of such organelles in male gametocytes of *P. berghei* has been recently described (9).

The confirmed organellar localization of the candidate proteins described here suggests that other OB components are potentially present in the list of the 16 upregulated OBC proteins. Candidates with signal peptide and transmembrane domains remain to be explored, including the non-annotated PF3D7_1222100 gene product, the putative signal peptidase complex subunit 3, SPC3 (PF3D7_0904400) and the GPI-anchored antigen PfGAMA (PF3D7_0828800). PfGAMA has been characterized in asexual parasites as a specific component of the micronemes (49), present on the merozoite surface after secretion from these organelles, and its expression was described also in ookinetes and sporozoites, the other invasive stages of the parasite (49,50). This draws a parallelism with PfSUB2 and suggests that the storage organelle of PfGAMA in the sexual stages could be the OBs, an hypothesis to be explored with available specific antibodies (50). Interestingly, gene disruption of the murine parasite *pfGAMA* ortholog, named *pbPSOP9*, phenotypically resulted in parasites with a reduced oocyst and sporozoite production, in which mosquito transmission to the mouse was abolished (51). Another shortlisted protein, RAB5b, is part of the rab GTPase protein family, associated to membrane trafficking (52). This points to a possible role of RAB5b in trafficking of components of the OBs to their cellular target.

Results of the present study expand our knowledge of the secretory organelles of *P. falciparum* by identifying novel proteins specific to the gametocyte OBs. The persistence in the extracellular gametes of the *P. falciparum* SUB2 and DPAP2 proteases, assigned here to these organelles, and the indication that OBs and their specific component Pfg377 are necessary to efficient oocyst formation identify a function of OBs in *P. falciparum* infection to mosquitoes and indicate OBs and their components as new targets for disrupting malaria transmission.

REFERENCES

11. WHO. (2015) World Malaria Report 2015

2. Arai, M., Billker, O., Morris, H.R., Panico, M., Delcroix, M., Dixon, D., Ley, S. V, and Sinden, R.E. (2001) Both mosquito-derived xanthurenic acid and a host blood-derived factor regulate gametogenesis of Plasmodium in the midgut of the mosquito. *Mol. Biochem. Parasitol.* **116**, 17–24

3. Kuehn, A., and Pradel, G. (2010) The coming-out of malaria gametocytes. *J. Biomed. Biotechnol.* **2010**

4. Blackman, M.J., and Bannister, L.H. (2001) Apical organelles of Apicomplexa: biology and isolation by subcellular fractionation. *Mol. Biochem. Parasitol.* **117**, 11–25

5. De Souza, W. (2006) Secretory organelles of pathogenic protozoa. *An. Acad. Bras. Cienc.* **78**, 271–291

6. Cowman, A.F., Berry, D., and Baum, J. (2012) The cellular and molecular basis for malaria parasite invasion of the human red blood cell. *J. Cell Biol.* **198**, 961–71

7. Singh, S., Plassmeyer, M., Gaur, D., and Miller, L.H. (2007) Mononeme: a new secretory organelle in Plasmodium falciparum merozoites identified by localization of rhomboid-1 protease. *Proc. Natl. Acad. Sci. U. S. A.* **104**, 20043–8

8. Yeoh, S., O'Donnell, R. a, Koussis, K., Dluzewski, A.R., Ansell, K.H., Osborne, S. a, Hackett, F., Withers-Martinez, C., Mitchell, G.H., Bannister, L.H., Bryans, J.S., Kettleborough, C. a, and Blackman, M.J. (2007) Subcellular discharge of a serine protease mediates release of invasive malaria parasites from host erythrocytes. *Cell*. **131**, 1072–83

9. Olivieri, A., Bertuccini, L., Deligianni, E., Franke-Fayard, B., Curr??, C., Siden-Kiamos, I., Hanssen, E., Grasso, F., Superti, F., Pace, T., Fratini, F., Janse, C.J., Ponzi, M., Currà, C., Siden-Kiamos, I., Hanssen, E., Grasso, F., Superti, F., Pace, T., et al. (2014) Distinct properties of the egress-related osmiophilic bodies in male and female gametocytes of the rodent malaria parasite Plasmodium berghei. *Cell. Microbiol.* **17**, 1–28

10. Alano, P., Read, D., Bruce, M., Aikawa, M., Kaido, T., Tegoshi, T., Bhatti, S., Smith, D.K., Luo, C., Hansra, S., Carter, R., and Elliott, J.F. (1995) COS cell expression cloning of Pfg377, a Plasmodium falciparum gametocyte antigen associated with osmiophilic bodies. *Mol. Biochem. Parasitol.* **74**, 143–56

11. Talman, A.M., Lacroix, C., Marques, S.R., Blagborough, A.M., Carzaniga, R., Ménard, R., and Sinden, R.E. (2011) PbGEST mediates malaria transmission to both mosquito and vertebrate host. *Mol. Microbiol.* **82**, 462–474

12. Ponzi, M., Sidén-Kiamos, I., Bertuccini, L., Currà, C., Kroeze, H., Camarda, G., Pace, T., Franke-Fayard, B., Laurentino, E.C., Louis, C., Waters, A.P., Janse, C.J., and Alano, P. (2009) Egress of Plasmodium berghei gametes from their host erythrocyte is mediated by the MDV-1/PEG3 protein. *Cell. Microbiol.* **11**, 1272–88

13. Furuya, T., Mu, J., Hayton, K., Liu, A., Duan, J., Nkrumah, L., Joy, D. a, Fidock, D. a, Fujioka, H., Vaidya, A.B., Wellems, T.E., and Su, X. (2005) Disruption of a Plasmodium falciparum gene linked to male sexual development causes early arrest in

gametocytogenesis. *Proc. Natl. Acad. Sci. U. S. A.* **102**, 16813–8

14. Lanfrancotti, A., Bertuccini, L., Silvestrini, F., and Alano, P. (2007) Plasmodium falciparum: mRNA co-expression and protein co-localisation of two gene products upregulated in early gametocytes. *Exp. Parasitol.* **116**, 497–503

15. Suárez-Cortés, P., Silvestrini, F., and Alano, P. (2014) A fast, non-invasive, quantitative staining protocol provides insights in Plasmodium falciparum gamete egress and in the role of osmiophilic bodies. *Malar. J.* **13**, 389

16. de Koning-Ward, T.F., Olivieri, A., Bertuccini, L., Hood, A., Silvestrini, F., Charvalias, K., Berzosa Díaz, P., Camarda, G., McElwain, T.F., Papenfuss, T., Healer, J., Baldassarri, L., Crabb, B.S., Alano, P., and Ranford-Cartwright, L.C. (2008) The role of osmiophilic bodies and Pfg377 expression in female gametocyte emergence and mosquito infectivity in the human malaria parasite Plasmodium falciparum. *Mol. Microbiol.* **67**, 278–90

17. Yeh, E., and DeRisi, J.L. (2011) Chemical rescue of malaria parasites lacking an apicoplast defines organelle function in blood-stage plasmodium falciparum. *PLoS Biol.* **9**

18. Lasonder, E., Rijpma, S.R., van Schaijk, B.C.L., Hoeijmakers, W.A.M., Kensche, P.R., Gresnigt, M.S., Italiaander, A., Vos, M.W., Woestenenk, R., Bousema, T., Mair, G.R., Khan, S.M., Janse, C.J., Bártfai, R., and Sauerwein, R.W. (2016) Integrated transcriptomic and proteomic analyses of P. falciparum gametocytes: molecular insight into sex-specific processes and translational repression. *Nucleic Acids Res.*

19. Walliker, D., Quakyi, I., Wellems, T., McCutchan, T., Szarfman, A., London, W., Corcoran, L., Burkot, T., and Carter, R. (1987) Genetic analysis of the human malaria parasite Plasmodium falciparum. *Science (80-.).* **236**, 1661–1666

20. Silvestrini, F., Tibúrcio, M., Bertuccini, L., and Alano, P. (2012) Differential adhesive properties of sequestered asexual and sexual stages of Plasmodium falciparum on human endothelial cells are tissue independent. *PLoS One*. **7**, e31567

21. Ljungström, I., Perlmann, H., Schlichtherle, M., Scherf, A., and Wahlgren, M. (2013) Methods in malaria research, 6th edition

22. Fidock, D. a, and Wellems, T.E. (1997) Transformation with human dihydrofolate reductase renders malaria parasites insensitive to WR99210 but does not affect the intrinsic activity of proguanil. *Proc. Natl. Acad. Sci. U. S. A.* **94**, 10931–10936

23. Duraisingh, M.T., Triglia, T., and Cowman, A.F. (2002) Negative selection of Plasmodium falciparum reveals targeted gene deletion by double crossover recombination. *Int. J. Parasitol.* **32**, 81–9

24. Lasonder, E., Ishihama, Y., Andersen, J.S., Vermunt, A.M.W., Pain, A., Sauerwein, R.W., Eling, W.M.C., Hall, N., Waters, A.P., Stunnenberg, H.G., and Mann, M. (2002) Analysis of the Plasmodium falciparum proteome by high-accuracy mass spectrometry. *Nature*. **419**, 537–42

25. Rappsilber, J., Ishihama, Y., and Mann, M. (2003) Stop and Go Extraction Tips for Matrix-Assisted Laser Desorption / Ionization , Nanoelectrospray , and LC / MS Sample Pretreatment in Proteomics. *Anal. Chem.* **75**, 663–670

26. Cox, J., Neuhauser, N., Michalski, A., Scheltema, R. a., Olsen, J. V., and Mann, M. (2011) Andromeda: A peptide search engine integrated into the MaxQuant environment. *J. Proteome Res.* **10**, 1794–1805

27. Cox, J., and Mann, M. (2008) MaxQuant enables high peptide identification rates, individualized p.p.b.-range mass accuracies and proteome-wide protein quantification. *Nat. Biotechnol.* , 1367–1372

28. Luber, C. a, Cox, J., Lauterbach, H., Fancke, B., Selbach, M., Tschopp, J., Akira, S., Wiegand, M., Hochrein, H., O'Keeffe, M., and Mann, M. (2010) Quantitative proteomics reveals subset-specific viral recognition in dendritic cells. *Immunity*. **32**, 279–89

29. Cox, J., Hein, M.Y., Luber, C. a., Paron, I., Nagaraj, N., and Mann, M. (2014) Accurate Proteome-wide Label-free Quantification by Delayed Normalization and Maximal Peptide Ratio Extraction, Termed MaxLFQ. *Mol. Cell. Proteomics*. **13**, 2513–2526

30. Cox, J., and Mann, M. (2012) 1D and 2D annotation enrichment: a statistical method integrating quantitative proteomics with complementary high-throughput data. *BMC Bioinformatics*. **13**, S12

31. Silvestrini, F., Lasonder, E., Olivieri, A., Camarda, G., van Schaijk, B., Sanchez, M., Younis Younis, S., Sauerwein, R., and Alano, P. (2010) Protein export marks the early phase of gametocytogenesis of the human malaria parasite Plasmodium falciparum. *Mol. Cell. Proteomics*. **9**, 1437–1448

32. Vizcaíno, J.A., Csordas, A., Del-Toro, N., Dianes, J.A., Griss, J., Lavidas, I., Mayer, G., Perez-Riverol, Y., Reisinger, F., Ternent, T., Xu, Q.-W., Wang, R., and Hermjakob, H. (2016) 2016 update of the PRIDE database and its related tools. *Nucleic Acids Res.* **44**, D447–56

33. Baker, D.A. (2010) Malaria gametocytogenesis. *Mol. Biochem. Parasitol.* **172**, 57–65

34. Young, J. a, Fivelman, Q.L., Blair, P.L., de la Vega, P., Le Roch, K.G., Zhou, Y., Carucci, D.J., Baker, D. a, and Winzeler, E. a. (2005) The Plasmodium falciparum sexual development transcriptome: a microarray analysis using ontology-based pattern identification. *Mol. Biochem. Parasitol.* **143**, 67–79

35. Costes, S. V, Daelemans, D., Cho, E.H., Dobbin, Z., Pavlakis, G., and Lockett, S. (2004) Automatic and quantitative measurement of protein-protein colocalization in live cells. *Biophys. J.* **86**, 3993–4003

36. Hackett, F., Sajid, M., Withers-Martinez, C., Grainger, M., and Blackman, M.J. (1999) PfSUB-2: A second subtilisin-like protein in Plasmodium falciparum merozoites. *Mol. Biochem. Parasitol.* **103**, 183–195

37. Olivieri, A., Collins, C.R., Hackett, F., Withers-Martinez, C., Marshall, J., Flynn, H.R., Skehel, J.M., and Blackman, M.J. (2011) Juxtamembrane shedding of Plasmodium falciparum AMA1 is sequence independent and essential, and helps evade invasion-inhibitory antibodies. *PLoS Pathog.* **7**, e1002448

38. Tanaka, T.Q., Deu, E., Molina-Cruz, A., Ashburne, M.J., Ali, O., Suri, A., Kortagere, S., Bogyo, M., and Williamson, K.C. (2013) Plasmodium dipeptidyl aminopeptidases as malaria transmission-blocking drug targets. *Antimicrob. Agents Chemother.* **57**, 4645–52

39. Sala, K.A., Nishiura, H., Upton, L.M., Zakutansky, S.E., Delves, M.J., Iyori, M., Mizutani, M., Sinden, R.E., Yoshida, S., and Blagborough, A.M. (2015) The Plasmodium berghei sexual stage antigen PSOP12 induces anti-malarial transmission blocking immunity both in vivo and in vitro. *Vaccine*. Elsevier Ltd; **33**, 437–445

40. Child, M. a, Harris, P.K., Collins, C.R., Withers-Martinez, C., Yeoh, S., and Blackman, M.J. (2013) Molecular determinants for subcellular trafficking of the malarial sheddase

PfSUB2. *Traffic*. **14**, 1053–64

41. Harris, P.K., Yeoh, S., Dluzewski, A.R., O'Donnell, R. a, Withers-Martinez, C., Hackett, F., Bannister, L.H., Mitchell, G.H., and Blackman, M.J. (2005) Molecular identification of a malaria merozoite surface sheddase. *PLoS Pathog.* **1**, 241–51

42. Green, J.L., Hinds, L., Grainger, M., Knuepfer, E., and Holder, A.A. (2006) Plasmodium thrombospondin related apical merozoite protein (PTRAMP) is shed from the surface of merozoites by PfSUB2 upon invasion of erythrocytes. *Mol. Biochem. Parasitol.* **150**, 114–117

43. Uzureau, P., Barale, J.-C., Janse, C.J., Waters, A.P., and Breton, C.B. (2004) Gene targeting demonstrates that the Plasmodium berghei subtilisin PbSUB2 is essential for red cell invasion and reveals spontaneous genetic recombination events. *Cell. Microbiol.* **6**, 65–78

44. Withers-Martinez, C., Jean, L., and Blackman, M.J. (2004) Subtilisin-like proteases of the malaria parasite. *Mol. Microbiol.* **53**, 55–63

45. Han, Y.S., Thompson, J., Kafatos, F.C., and Barillas-Mury, C. (2000) Molecular interactions between Anopheles stephensi midgut cells and Plasmodium berghei: The time bomb theory of ookinete invasion. *EMBO J.* **95**, 6030–6040

46. Ghorbal, M., Gorman, M., Macpherson, C.R., Martins, R.M., Scherf, A., and Lopez-Rubio, J.-J. (2014) Genome editing in the human malaria parasite Plasmodium falciparum using the CRISPR-Cas9 system. *Nat. Biotechnol.* **32**

47. Jones, M.L., Das, S., Belda, H., Collins, C.R., Blackman, M.J., and Treeck, M. (2016) A versatile strategy for rapid conditional genome engineering using loxP sites in a small synthetic intron in Plasmodium falciparum. *Sci. Rep.* Nature Publishing Group; **6**, 21800

48. Arastu-Kapur, S., Ponder, E.L., Fonović, U.P., Yeoh, S., Yuan, F., Fonović, M., Grainger, M., Phillips, C.I., Powers, J.C., and Bogyo, M. (2008) Identification of proteases that regulate erythrocyte rupture by the malaria parasite Plasmodium falciparum. *Nat. Chem. Biol.* **4**, 203–13

49. Arumugam, T.U., Takeo, S., Yamasaki, T., Thonkukiatkul, A., Miura, K., Otsuki, H., Zhou, H., Long, C. a, Sattabongkot, J., Thompson, J., Wilson, D.W., Beeson, J.G., Healer, J., Crabb, B.S., Cowman, A.F., Torii, M., and Tsuboi, T. (2011) Discovery of GAMA, a Plasmodium falciparum merozoite micronemal protein, as a novel blood-stage vaccine candidate antigen. *Infect. Immun.* **79**, 4523–32

50. Hinds, L., Green, J.L., Knuepfer, E., Grainger, M., and Holder, A. a. (2009) Novel putative glycosylphosphatidylinositol-anchored micronemal antigen of Plasmodium falciparum that binds to erythrocytes. *Eukaryot. Cell*. **8**, 1869–79

51. Ecker, A., Bushell, E.S.C., Tewari, R., and Sinden, R.E. (2008) Reverse genetics screen identifies six proteins important for malaria development in the mosquito. *Mol. Microbiol.* **70**, 209–20

52. Hutagalung, A.H., and Novick, P.J. (2011) Role of Rab GTPases in membrane traffic and cell physiology. *Physiol. Rev.* **91**, 119–49

53. Bahl, A., Brunk, B., Crabtree, J., Fraunholz, M.J., Gajria, B., Grant, G.R., Ginsburg, H., Gupta, D., Kissinger, J.C., Labo, P., Li, L., Mailman, M.D., Milgram, A.J., Pearson, D.S., Roos, D.S., Schug, J., Stoeckert, C.J., and Whetzel, P. (2003) PlasmoDB: The Plasmodium genome resource. A database integrating experimental and computational

data. *Nucleic Acids Res.* **31**, 212–215

FOOTNOTES

Acknowledgments.

This work was supported in part by the EU FP7 Network of Excellence ‘European Virtual Institute of Malaria Research EVIMalaR’ (Project n. 242095), the EU FP7 Project ‘OzMalNet’ (Project n. 269238) and the Bill & Melinda Gates Foundation Grant OPP1040394. Prof. G. Girelli, Blood Centre of ‘Sapienza’ University of Rome , and Mr L. Picci, Istituto Superiore di Sanità, are acknowledged for the gift of human red blood cells and for mouse immunization, respectively.

This article contains supplemental Experimental Procedures, Figures S1–S12 and Tables S1–S9.

FIGURE LEGENDS

FIG. 1. **Characterization of independent *pfg377*KO parasite clones.**

A: Ultrastructural sections of *wt* and *pfg377*KO 8-20 gametocytes. Scale bar: 2μM. B: IFA on acetone-fixed *wt* and *pfg377*KO 8-20 gametocytes using rabbit α-Pfg377B (1:800 dilution) antibodies. Scale bar: 5μM. BF: bright field. C: Western blot analysis on stage V gametocytes of the *wt* and *pfg377*KO clones 5-2 and 8-20 using α-Pfg377-B antibodies (1:5000 dilution) and a rabbit α-Pfg27 antibody (1:3000 dilution) as loading control. $5x10^5$ parasites or RBCs were loaded per lane. D: Egress efficiency of gametocytes from *wt* and *pfg377*KO clones 5-2 and 8-20. Paired t tests comparing egress efficiency of *wt* gametocytes to gametocytes from clones 5-2 ($p=0.249$) and 8-20 ($p=0.21$) were performed. N:4, n:200, error bar: SD. E: Wt and *pfg377*KO (clone 5-2) parasite survival in *A. gambiae* mosquitoes. Oocysts numbers (upper panel) and prevalence of infection (lower panel) are shown. (N:4, n:118), details in Table S2.

FIG. 2. **Differentially expressed proteins in *wt* and Pfg377 defective gametocytes by label free quantitative proteomics.**

Volcano plot representation of differentially expressed proteins in *wt* and Pfg377-deficient gametocytes identifies proteins overrepresented (red dots) and underrepresented (black dots) in *wt* and Pfg377 deficient gametocytes over the majority of proteins with unchanged abundance levels (grey dots). The dot corresponding to Pfg377, at far right tail of the Volcano plot ($x=10.43$, $y=81.74$), is not shown.

FIG. 3. **PfGEST localization in the *P. falciparum* gametocyte osmiophilic bodies.**

A. Western blot analysis with mouse α-PfGEST antibodies (1:1000 dilution) on the indicated parasite stages. Rabbit α-Pfg27 antibodies (1:3000 dilution) were used as loading control. $5x10^5$ parasites or uninfected RBCs (uRBC) were loaded per lane. g: gametocytes. B: IFA on acetone-fixed *wt* gametocytes using mouse α-PfGEST (1:100 dilution) and rabbit α-Pfg377B (1:800 dilution) antibodies. Scale bar: 5μM. BF: bright field. C. Representative immunoelectron micrograph showing the localization of PfGEST specific gold particles (α-PfGEST primary antibody 1:100 dilution) on the electrondense OB structures in sections from *wt* gametocytes. Scale bar: 1μM.

FIG. 4. **Expression and OB localization of the PfSUB2-, PfDPAP2- and PfOBC13-GFP fusions in late gametocytes.**

A: GFP fluorescence of live gametocytes from the lines indicated. B: IFA experiments with α-GFP (rabbit, 1: 100, green) used alone or in combination with rat α-Pfg377-A2 (1:200 dilution) antibodies on gametocytes from the lines indicated. BF: bright field. Scale bar: 5 μM.

FIG. 5. **Egress efficiency of *pfDPAP2KO* and *pfOBC13KO* gametes.**

Egress efficiency of gametocytes from the *pfDPAP2*KO clones E10 and T5 and the *pfobc13*KO clone 1. N:4, n:200. Error bar: SD.

FIG. 6. **Fluorescence of *OBC-GFP* fusion proteins in live gametes after egress from host RBC.**

RBCs infected with stage V gametocytes from *wt* and from the transgenic lines indicated were surface stained with fluorophore-conjugated WGA before parasites were activated with XA to undergo gametogenesis. Live gametes were then inspected for GFP fluorescence and scored

for the presence or absence of WGA surface fluorescence, respectively diagnostic of presence or absence of the host RBC. BF: bright field. Scale bar: 5 μM. WGA: Alexa fluor 594-WGA.

FIG. 1. **Characterization of independent *pfg377*KO parasite clones.**

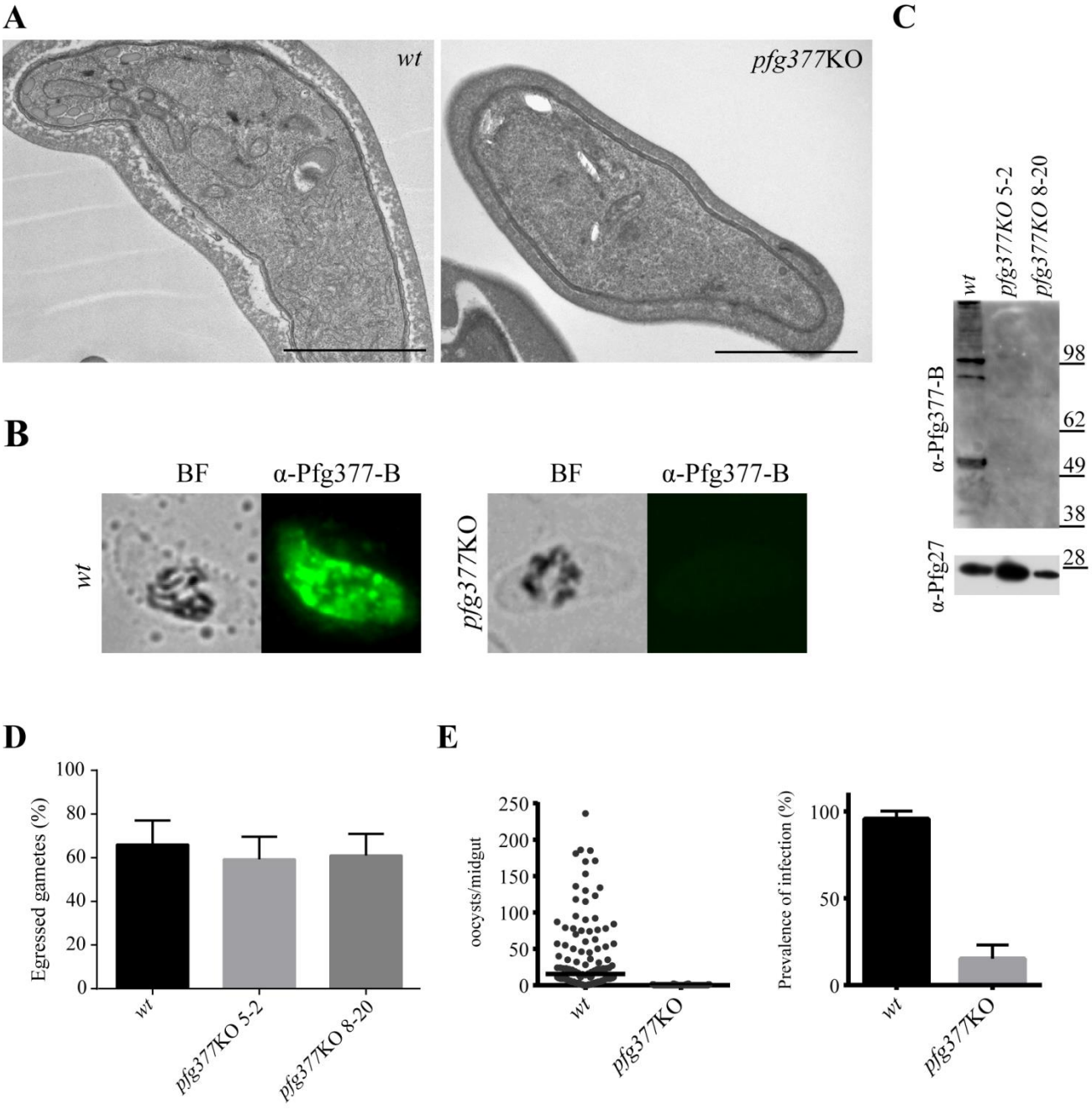

FIG. 2. **Differentially expressed proteins in *wt* and Pfg377 defective gametocytes by label free quantitative proteomics.**

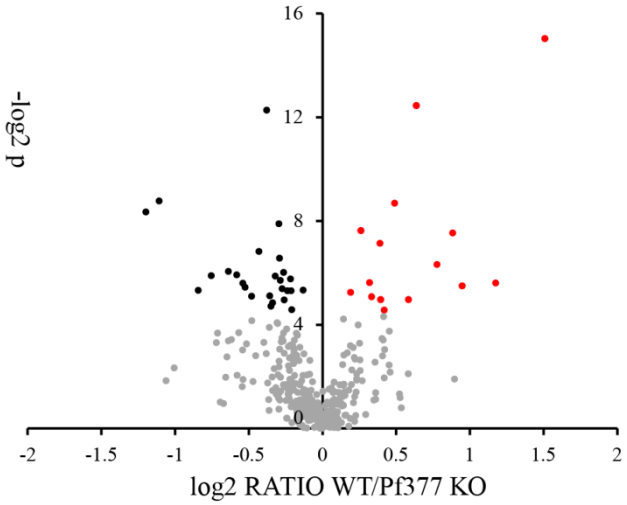

FIG. 3. **PfGEST localization in the *P. falciparum* gametocyte osmiophilic bodies.**

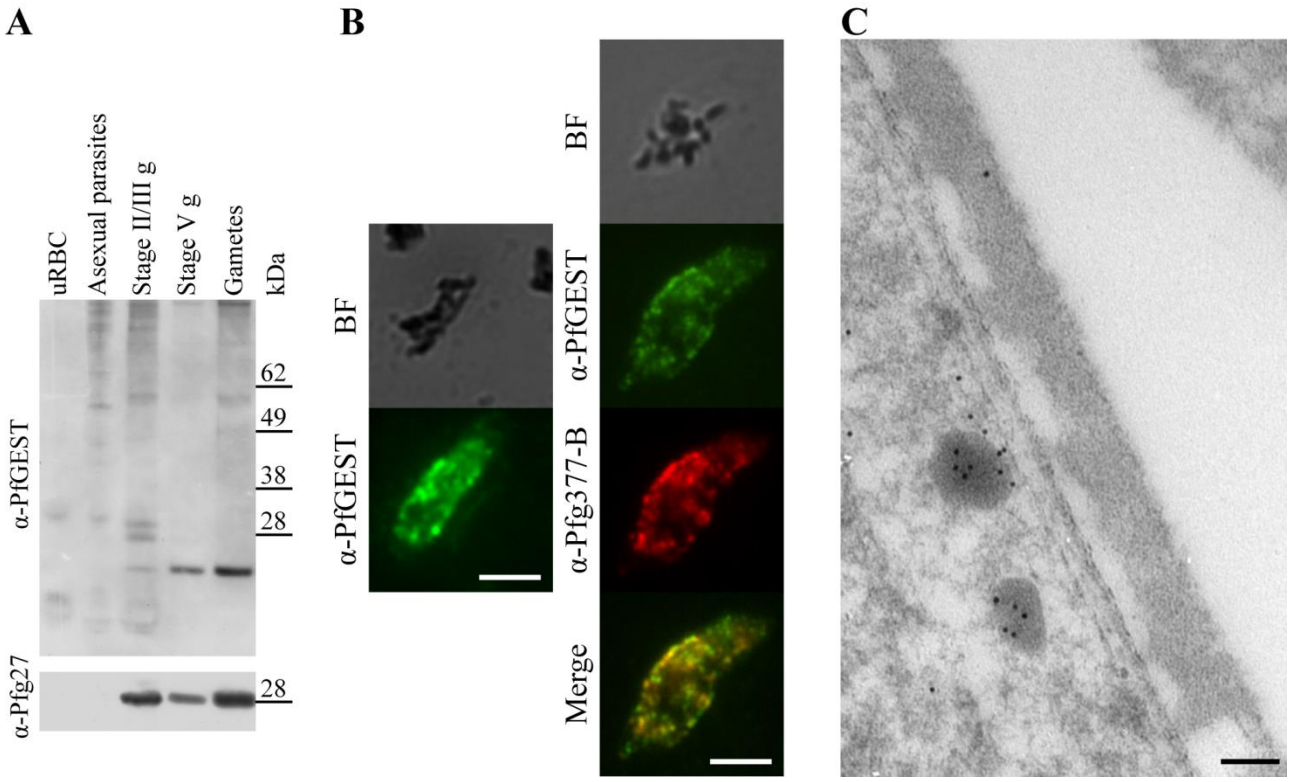

FIG. 4. **Expression and OB localization of the PfSUB2-, PfDPAP2- and PfOBC13-GFP fusions in late gametocytes.**

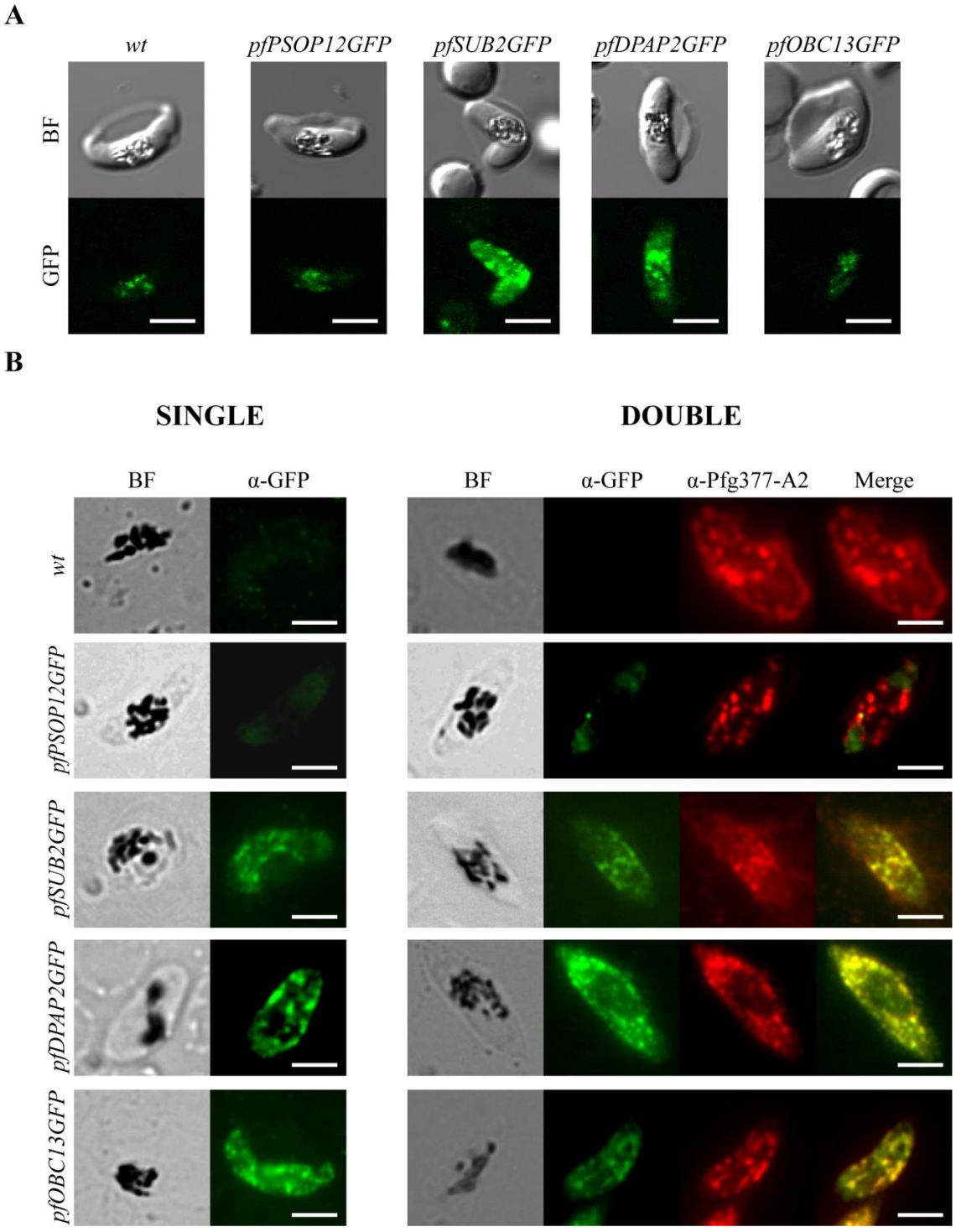

FIG. 5. **Egress efficiency of *pfDPAP2KO* and *pfOBC13KO* gametes.**

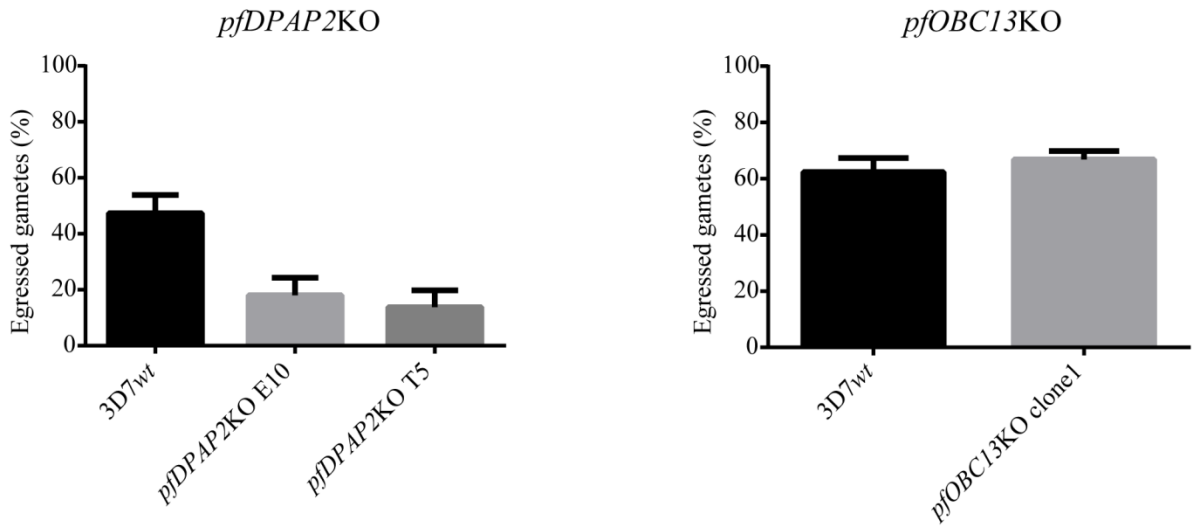

FIG. 6. **Fluorescence of *OBC-GFP* fusion proteins in live gametes after egress from host RBC.**

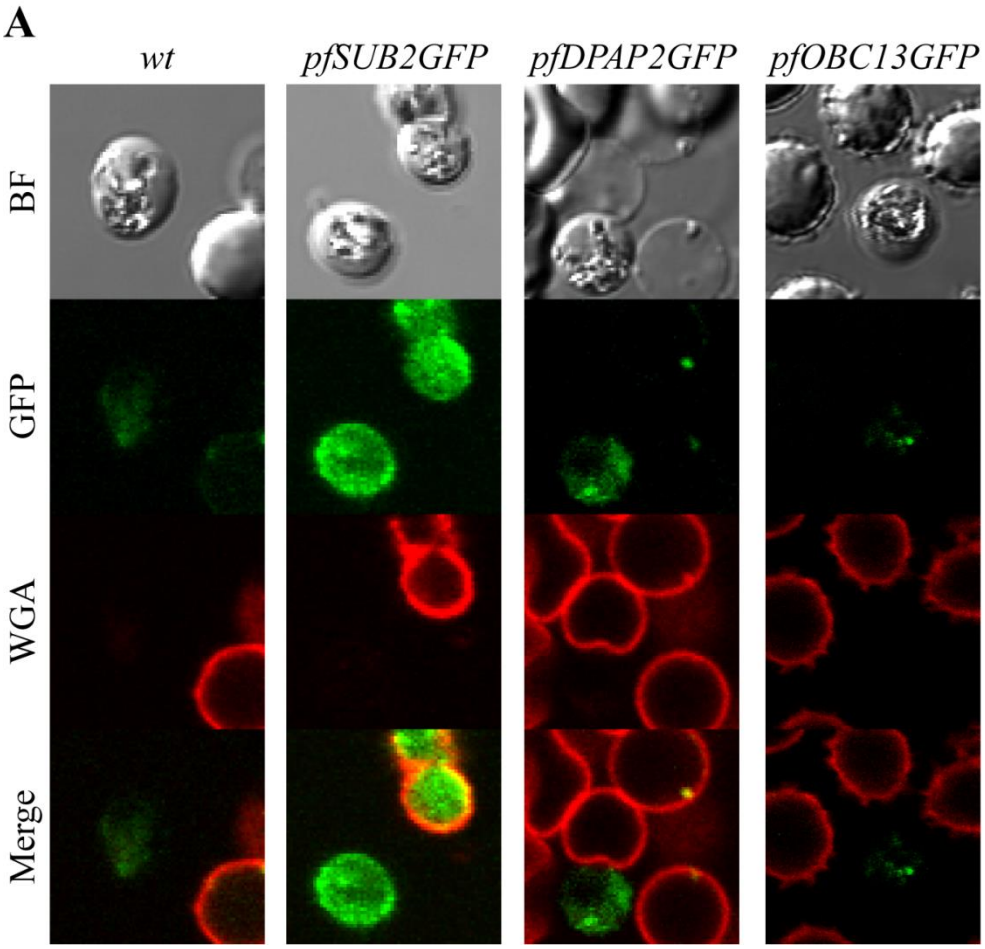

TABLES

TABLE 1. Proteins overrepresented in *wt* vs *pfg377KO* gametocytes.

Proteins significantly (t-test positive) overrepresented in *wt* vs *pfg377KO* gametocytes with the respective average abundance $\log_2$ ratios. ID and annotation from PlasmoDB database, release 28 (http://plasmodb.org/plasmo/) (53).

Protein ID	Protein Name	$\log_2$ ratio *wtl pfg377KO*
PF3D7_1250100	osmiophilic body protein (G377)	10.43
PF3D7_1136900	subtilisin-like protease 2 (SUB2)	1.51
PF3D7_1247800	dipeptidyl aminopeptidase 2 (DPAP2)	1.18
PF3D7_0904400	signal peptidase complex subunit 3, putative (SPC3)	0.95
PF3D7_0828800	GPI-anchored micronemal antigen (GAMA)	0.89
PF3D7_1222100	conserved Plasmodium protein, unknown function	0.77
PF3D7_0513700	secreted ookinete protein, putative (PSOP12)	0.63
PF3D7_1449000	gamete egress and sporozoite traversal protein, putative (GEST)	0.58
PF3D7_1310600	ras-related protein Rab-5B (RAB5b)	0.49
PF3D7_1328100	proteasome subunit beta type-7, putative	0.42
PF3D7_0204900	ubiE/COQ5 methyltransferase, putative	0.39
PF3D7_0517600	F-actin-capping protein subunit beta, putative (CPbeta)	0.39
PF3D7_0813200	CS domain protein, putative	0.33
PF3D7_0209200	3’ exoribonuclease, putative	0.32
PF3D7_0412200	conserved Plasmodium protein, unknown function	0.26
PF3D7_0629800	cullin-like protein, putative	0.19